ELSEVIER

Contents lists available at ScienceDirect

Nano Energy

journal homepage: www.elsevier.com/locate/nanoen



A dual-electrolyte based air-breathing regenerative microfluidic fuel cell with 1.76 V open-circuit-voltage and 0.74 V water-splitting voltage



Haiyang Zou a,b,*, Jun Chen , Yunnan Fang Jilai Ding , Wenbo Peng , Ruiyuan Liu

- a School of Materials Science and Engineering, Georgia Institute of Technology, Atlanta, GA 30332, USA
- ^b Department of Mechanical Engineering, The University of Hong Kong, Hong Kong

ARTICLE INFO

Article history:
Received 1 June 2016
Received in revised form
18 July 2016
Accepted 27 July 2016
Available online 6 August 2016

Keywords: Regenerative fuel cell Microfluidic fuel cell Water split Dual electrolyte Neutralization energy

ABSTRACT

The open circuit voltage of a conventional H_2 - O_2 fuel cell is limited to $\sim 1.23~V$ under atmospheric pressure, which limits the efficiency of the system. Here, we reported a dual-electrolyte microfluidic fuel cell system (DEFC), which could stably deliver an open circuit voltage up to 1.76 V at room temperature under atmospheric pressure, and a peak power density of 145 mW/cm², improved by 3 times compared with that in single electrolyte mode. When operated in the reverse mode, the microfluidic cell can be used for water electrolysis, demonstrating a water split voltage of $\sim 0.74~V$ and a round trip voltage efficiency of 83.5% at a current density of $100~mA/cm^2$. The neutralization energy of the two electrolytes, which could be wasted as heat, can be directly utilized to produce electricity or split water with high efficiency. Given the DEFC's features of high open-circuit voltage, low water splitting voltage, and room-temperature operation condition, the reported DEFCs technology presents a superior route for high-efficiency energy conversion and storage system that could revolutionize the fields of large-scale energy storage and portable power systems.

© 2016 Elsevier Ltd. All rights reserved.

1. Introduction

With the aggravating greenhouse effect due to the increased carbon emissions and the limited fossil energy available for the next century, searching renewable and clean energy technologies is mandatory for the sustainable development of human civilization [1–7]. Fuel cells (FCs) are being widely investigated and attracting increasing scientific attentions owning to their high efficiency and energy density, silent operation, great sustainability, environmentfriendly, continuous power supply and trouble-free recycling [8–14]. However, due to the thermodynamic limitation, the highest possible open circuit voltage (OCV) of a traditional FC is 1,23 V, and stacking of such FCs to boost the output to a practical level usually results in a large physical size and high cost. In addition, the high operation temperature has largely hindered the application of traditional FCs as a mobile power source for microelectrochemical systems [15–18]. Therefore, fabricating micro fuel cells is not just a matter of downsizing the cell dimensions and improving the power generation capabilities, but also addressing these aforementioned issues, and developing new materials and novel conceptual designs for microscale fuel cells at low temperature and pressure.

Microfluidic fuel cells, whose electrolyte, reactions sites and electrodes are all confined to micro channels, have been proposed to address many of the challenges that face traditional membranebased systems [19-25]. This type of fuel cells operate at room temperature without a physical barrier, such as a membrane, therefore decrease the cost, relax hydration requirements and open up the possibility for a much wider range of chemistries to be studied, like vanadium redox flow batteries [18,22], methanol [21], formic acid [20], hydrogen fuel cells, and hydrogen bromine [26]. Among these systems, hydrogen fuels cells are expected to be the best choice in terms of availability. Using air-breathing cathodes seems to be another promising microfluidic fuel cell design for some practical operations [21]. The development of microfluidic fuel cells has been tremendous, resulted in operational devices with promising performance at room temperature in terms of power density and cell voltage, but their low energy density is the most prominent constraint for current microfluidic fuel cells.

Here, in this study, we reported a dual electrolyte based FC (DEFC) with air-breathing and its novel application as a regenerative fuel cell. We presented a simple conceptual model-membraneless microfluidic device to test the DEFC performance. In our designed cell topology, the co-laminar configuration allowed the anolyte and catholyte streams to flow separately in parallel between gas diffusion electrodes. By introducing a pH gradient between electrodes in fuel cell mode (FC mode), a high open circuit voltage of up to 1.76 V and a power density of

^{*} Corresponding author at: School of Materials Science and Engineering, Georgia Institute of Technology, Atlanta, GA 30332, USA. E-mail address: hzou8@gatech.edu (H. Zou).

145 mW/cm² were generated at room temperature under atmospheric pressure, which were respectively about 1.46-1.75 times and 3 times higher than those of the single electrolyte based FCs under the same conditions. Furthermore, the advantage of shifting oxidation and reduction potential was taken in the water electrolysis mode (WE mode) to reduce the water splitting voltage, so that more sources of waste electricity at a low voltage were able to be utilized. The presented DEFC achieved a water splitting voltage \sim 0.74 V, only about half of that in single electrolyte system, corresponding to a round trip voltage efficiency of as high as 83.5% at a current density of 100 mA/cm², which was well over that of other types of regenerative fuel cells (RFCs) [27–30]. Given a collection of compelling features of DEFCs, such as low-cost, roomtemperature operation, high open-circuit voltage, low water splitting voltage, no waste and without oxygen supply system, high specific density, longer-term energy storage, no limit capacity (without frequent charging), and insensitivity to cycle life, temperature or self-discharge [31-39], the DEFCs technology not only presents a superior route for high-efficiency water splitting, but also renders a green and environmentally friendly power source for portable electronics. It will have extensive applications with promising future in power generation and storage systems.

2. Experimental Section

2.1. Cell fabrication

The gas diffusion electrodes (Hispec 6000), made with catalyst PtRu Black (Johson Mattey, molar ratio of Pt/Ru=1:1, 10 mg/cm², XRD crystallite size < 4 nm) on carbon paper, were purchased from Hesen Co., Ltd., Shanghai, China. Details of channel dimensions and assemble information are shown in the supplementary material (Fig. S2). Briefly, the electrodes were placed in the engraved frame PMMA plates with open windows (1.5 mm × 3.3 mm) on opposing sides of two channels (Fig. S2). The components of the DEFC devices were manufactured by a carbon dioxide laser ablation system (VLS 2.30, Universal Laser System), and assembled manually. A chamber with dimensions of 53 mm $(L) \times 10 \text{ mm}(W) \times 5 \text{ mm}(H)$ was shaped by using the PMMA plate as a gas reservoir to store hydrogen. The thickness of channels was about 1 mm. The laminar flow sector was fabricated by taping all the PMMA plates together with double-sided adhesive tape. This sector was then clamped by a binder clip with two electrodes and two pieces of carbon cloth acted as current collector at each side (Fig. S2). To test the gas leakage for safety, the fabricated cell was immersed into the water, and then the air was pressed through the gas channels to check the gas bubbles in the water (Fig. S4). Through tests, such fabricated cells were proved to be well airtight without liquid leakage. Laminar flows were also verified by experiments described in the supplementary material (Fig. S3).

2.2. Electrochemical performance tests

The electrolyte solutions of 0.5 M $\rm H_2SO_4$ and 1 M KOH were prepared in DI water of 18.2 M Ω -cm. An electrochemical station (CHI 660E, CH Instruments, Inc.) was used to control the current and voltage applied to the cells, and collect data. The flow speed of electrolytes was controlled by a syringe pump (LSP02–1B, Longer Pump) at 600 μ L min $^{-1}$. All experiments were performed at room temperature under atmospheric pressure. The performance of single electrolyte systems was tested to be compared with that of the DEFC. For the single electrolyte system, the same electrolyte was pumped into the two channels; for the DEFCs, the alkali electrolyte flowed at the side of the hydrogen electrode, and the acid electrolyte flowed at the side of oxygen/air electrode. In FC

mode, H_2 (\geq 99.995%, *Linde*) was fed at a constant rate of 0.06 slpm (standard liter per minutes). In WE mode, for the DEFC, 0.5 M H_2SO_4 was pumped into the anode side channel to produce H_2 , and 1 M KOH was pumped into the cathode side channel to generate O_2 . Each data point was collected by integration after 60 s of steady-state operation to eliminate transient artifacts. Potentials of each individual electrode were recorded with digital multi-meters (Fluke) connected between each electrode and an external Ag/AgCl reference electrode in the electrolyte stream.

3. Results and discussion

3.1. System design and working principles

From thermodynamics, according to the Nernst equation, the two half-cell reactions taking place at two separate electrode sides and potentials with pH dependence can be expressed as follows:

$$2H^+ + 2e^- \leftrightarrow H_2 \tag{1}$$

$$E_{H^{+}/H_{2}} = E_{H^{+}/H_{2}}^{\circ} + \frac{RT}{2F} ln \left[\frac{(a_{H^{+}})^{2}}{a_{H_{2}}} \right] = 0 - 0.059V(pH)$$
 (2)

$$4H^+ + O_2 + 4e^- \leftrightarrow 2H_2O$$
 (3)

$$E_{O_2/H_2O} = E_{O_2/H_2O}^{\circ} + \frac{RT}{4F} ln \left[\frac{a_{O_2}(a_{H^+})^4}{(a_{H_2O})^2} \right] = 1.229 - 0.059 V(pH)$$
(4)

where E is the half-cell potential at the temperature of interest, E° is the standard half-cell potential, R is the universal gas constant, T is the absolute temperature at which the cell is operated, F is the Faraday constant, n is the number of moles of electrons transferred in the half-reaction, a is the chemical activity for the relevant species, and V(pH) is the pH value of the electrolyte in the half-cell.

The relationship between potentials of each electrode and pH of electrolyte can be illustrated in Fig. 1a. The potential difference of the electrodes remains a constant of 1.23 V (black solid circles), independent of the pH value of the electrolyte. Theoretically, this is the maximum OCV and the minimum water splitting voltage for a traditional H₂/O₂ fuel cell under atmospheric pressure. In order to improve the voltage output, a dual electrolyte based microfluidic FC was developed here. As illustrated in Fig. 1a, by placing the anode and cathode in two electrolytes with favorable pH environments, i.e., the oxygen electrode in acid (pH=0) and hydrogen electrode in alkaline (pH=14), the theoretical OCV of the aqueous electrochemical power source can reach up to 2.06 V (green arrows and solid circles); in the meanwhile, if the oxygen electrode is in alkaline (pH=14) and hydrogen electrode in acid (pH=0), the energy for water splitting can be minimized down to 0.4 V (blue arrows and solid circles).

To explore different combinations of the anodes and cathodes, the half-cell electrode reactions in FC mode and WE mode configuration are shown in Table 1. From the overall equations, we can find that in dual electrolyte system, neutralization reactions happen in both fuel cell and water electrolysis reactions. The higher voltage and additional energy can be interpreted as voltage energy

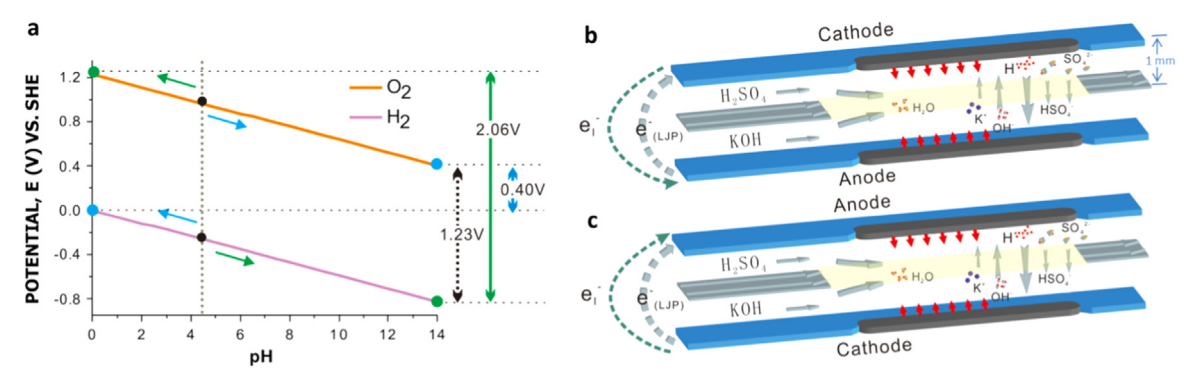


Fig. 1. Working principles of the DEFC. (a) Pourbaix diagram of H_2/O_2 at 25 °C and atmospheric pressure. Schematic view of single cell and diagram of the liquid junction potential setup at the fuel/oxidant interface: in FC mode (b) and in WE mode (c). Originally, the electrolytes in WE mode flow vertically from bottom to top to avoid the turbulence caused by bubble. For better comparison view, (c) is rotated right 90°. Arrows show the direction of net transfer for each ion, and their lengths indicate relative mobilities. The channels thickness is about 1 mm.

Table 1 Standard electrode potentials *versus* SHE of half-cell reactions and overall reactions in FC and WE mode for single and dual electrolyte. The acid employed is $0.5 \text{ M H}_2\text{SO}_4$ and the alkali is 1 M KOH.

		Single Electrolyte			Dual Electrolyte		
FC Mode	Acid	Anode:	$2H_2 - 4e \rightarrow 4H^+$	E = 0 A			
		Cathode:	$O_2 + 4e^- + 4H^+ \rightarrow 2H_2O$	E = 1.229 V	Cathode:	$O_2 + 4e^- + 4H^+ \rightarrow 2H_2O$	E = 1.229V
	Alkali	Anode:	$2H_2$ -4e + 4OH \rightarrow 4H ₂ O	E = -0.827 V	Anode:	$2H_2 - 4e^- + 4OH \rightarrow 4H_2O$	E = -0.827V
		Cathode:	$O_2 + 4e^- + 2H_2O \rightarrow 4OH^-$	E = 0.4 V			
Overall Reaction:			$2H_2 + O_2 \rightarrow 2H_2O$	E = 1.23 V	2H ₂ +C	$O_2 + 4OH^- + 4H^+ \rightarrow 6H_2O$	E = 2.06V
WE Mode	Acid	Anode:	$4H^+ + 4e^- \rightarrow 2H_2$	E = 0 V	Anode:	$4H^+ + 4e \rightarrow 2H_2$	E = 0V
		Cathode:	$2H_2O \rightarrow O_2 + 4e^- + 4H^+$	E = 1.229 V			
	Alkali	Anode:	$4H_2O + 4e^- \rightarrow 4OH^- + 2H_2$	E = -0.827 V			
		Cathode:	$4OH \rightarrow O_2 + 4e^- + 2H_2O$	E = 0.4 V	Cathode:	$4OH \rightarrow O_2 + 4e + 2H_2O$	E = 0.4V
Overall Reaction:			$2H_2O \rightarrow 2H_2 + O_2$	E = 1.23 V	4H ⁺ + 4	$OH \rightarrow O_2 + 2H_2 + 2H_2O$	E = 0.4V

from electrochemical neutralization. To verify this hypothesis, the cell voltage generated is calculated if the neutralization of acid and alkali solutions can be carried out electrochemically. The reaction in which hydroxide ions and protons combining to form water is

$$H^+ + 0H^- \leftrightarrow H_2 0 \tag{5}$$

and has a Gibbs free energy change of $\Delta G^o = -79.9$ kJ mol⁻¹ [40], corresponding to a voltage of 0.83 V under standard conditions [35] according to the Nernst equation. In FC mode, the potential 0.83 V provided from the neutralization reaction is applied to the electrodes and increases the potential between electrodes, thus improved the OCV; in WE mode, similarly, accompanied with producing hydrogen and oxygen, the additional potential generated from the neutralization reaction is also applied to the electrodes, so the external potential needed to be applied to the electrodes to split water can be reduced. Namely, the neutralization reaction energy could be utilized to produce electricity and break down water.

There was a liquid junction potential (LJP) associated with the dual electrolyte streams which was established due to the steep concentration gradients in ions and their largely different mobilities at the junction [41,42]. Fig. 1b illustrates the formation of the typical LJP between the alkaline anode stream and the acidic cathode stream in the system described. The LJP was contributed mostly by

H⁺ and OH⁻ ions as the mobility values of other ions (SO₄²-, HSO₄⁻, K⁺ etc.) were too low and very close to each other. On the basis of ion mobilities, the H⁺ ions have a larger mobility than OH⁻ ions, they initially penetrated the dilute phase at a higher rate, given a net positive charge to the dilute anode and a net negative charge to the concentrated cathode, with the result that a boundary potential difference was developed. The junction potential reduced the OCV (counter flow direction of electrons under the actions of liquid junction potential e_{LIP}^- and cell current e_I^-), as well as power generation in FC mode. Fig. 1c shows the typical liquid junctions in WE mode, which indicates that the LJP in this case could be expected to enhance the performance of the cell (same current flow direction of e_{IIP}^- and e_I^-). However, the LIP did not significantly contribute to the DEFC performance. Firstly, the maximum value for the LIP between 1 N H₂SO₄ and 1 N KOH alkali was estimated to be only 32 mV [43], and its effects on the cell performance was negligible; secondly, as the acid-alkali neutralization has 2-3 orders of magnitude higher rate constant than the diffusion rate of H⁺/OH⁻ ions, the H⁺ ions diffused across the interface area and neutralized the OH- ions which were self-diffused at opposite direction or brought by the flow, thus reducing the amount of charged mass transferred than normal situations, so that the value of LJP could be lower.

The co-laminar configuration in microchannels allowed the anolyte and catholyte streams to be selected independently (Fig. 1b and c), and it confined the neutralization reactions in the interface of the acid and alkali streams to small scale

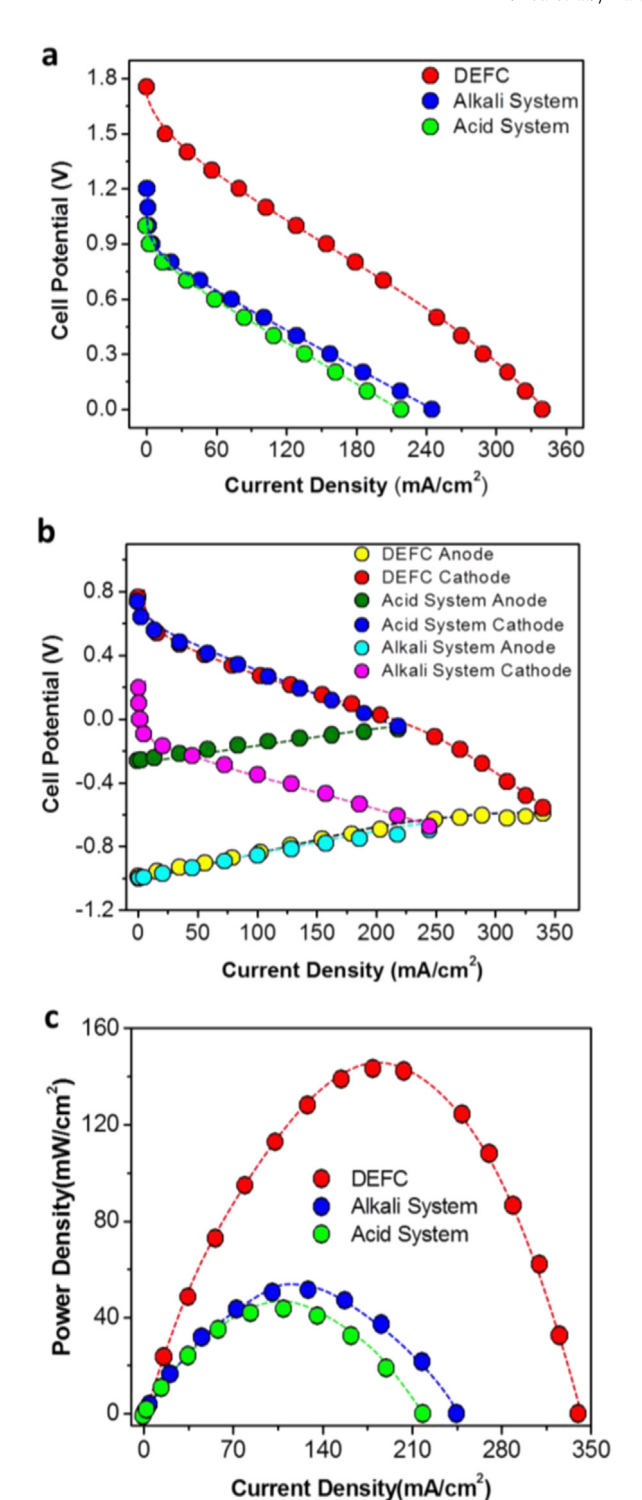


Fig. 2. Performance of the DEFCs in Fuel Cell Mode. (a) Load curves comparison among the DEFC, fuel cell in single alkali system and single acid system. (b) The corresponding U-I curves of individual electrode performances *versus* Ag/AgCl. (c) Power density curves comparison among the DEFC, fuel cell in single alkali system and single acid system.

[19,22,36,43,44], because of their momentum (the contact time of the two streams is too short to be mixed at large scales) and density difference (hydroxide ions are heavier than H⁺, so hydrogen ions flow can float at the upper layers which limits the diffusion of the two streams. When the alkali was located at the top, the dual electrolytes were proved experimentally to be mixed heavily at the interface between them). Microfluidic mixing process has been simulated through finite element modelling, which

is shown in the supplementary material (Fig. S5 and the gif pictures). The liquid-liquid interface was considered as a virtual membrane and ions travelled across the channel to reach the other side and completed the ionic conduction.

3.2. Fuel cell performance

As shown in Fig. 2a, the OCV was 1 V in the acid single electrolyte FC, 1.2 V in the alkali single electrolyte FC, but in the DEFC, it was 1.755 V, which was about 146-175% times as large as that in single electrolyte systems. The deviation from theoretical values in OCVs was primarily related to the large overpotential associated with the reduction of oxygen [44] and resistances in the fuel cell itself as well as some common issues referred to as small amount carbonation in alkali media (before or during the oxidation of the fuel, deleted) [45]. Besides, air contains only 20.95% oxygen, so the OCV was a bit lower than that when using pure oxygen. The overpotential of oxygen reduction in acid was larger than that in alkaline; this phenomenon has also been noticed and explained by others as the greater deleterious effect of the reaction kinetics than OH⁻ [46–48]. The maximum current density was 225 mA/cm² in the acid FC and 250 mA/cm² in alkali FC. For the DEFC, however, the maximum current density reached 350 mA/cm², which was an enhancement of 55% and 40% compared to that of the acid and alkali FC, respectively.

The corresponding voltage-current (U-I) curves of individual electrodes are shown in Fig. 2b. The curve of DEFC's cathode followed the same trend as that of the cathode in an acid single electrolyte system; anode followed the same trend as that of the anode in a single alkali system as expected. This fact demonstrated that the planar laminar flow sector successfully separated the dual electrolyte flows and also revealed that the half-cell reactions happened at each electrode (the same as Table 1). By combining the two half-cell reactions of the cathode in acid and the anode in alkali, we found that additional OCV of the DEFCs over single electrolyte based cell is from the neutralization reaction. However, the two half-cell reactions of the neutralization reaction took place at two electrodes, which are separated by flowing electrolytes and physically far from each other. Thus, the neutralization reaction energy was counted as the additional energy created at electrode sides, not from the interface between the two electrolytes. In most situations, neutralization of an acid and an alkali is carried out in the bulk and the energy released in the form of heat. These results revealed that electrochemical neutralization can proceed if protons are consumed at the cathode and hydroxide ions reacted separately at the anode, accompanied by electron transfer via an external circuit. As shown in Fig. 2b, as the current density increased from 250 to 300 mA/cm², the cell potential of anode side almost remained the same while the potential of the cathode side dropped, which indicated that the anode suffered less polarization losses compared with the cathode. Similar anode and cathode losses have been reported by others [49,50]. Mass transport-limited performance at high current density was not observed, which indicated that the proton concentration across the boundary layer and the rate of proton replenishment of the depletion boundary layer on the cathode was sufficient, and the air-breathing cathode had enough oxygen to consume.

As demonstrated in Fig. 2c, the DEFC produced a peak power density of 145 mW/cm² at about 0.8 V, which was about 3.6 times higher than that under that in acid single electrolyte condition which delivered a peak power density of 40 mW/cm² at 0.4 V; about 2.9 times higher than that under alkaline single electrolyte conditions, which was 50 mW/cm² at about 0.4 V. In summary, in FC mode, the OCV, current density and power density of the DEFC were all experimentally proved to be much higher than those of a FC in single electrolyte under the same conditions. In this mode,

the neutralization energy utilization efficiency was calculated in the <u>supplementary material</u>, which was about 8.8%. With one pump in microfluidic FC, stacking up a bunch of such DEFCs can provide a larger power than stacking up the same amount of cells in single electrolyte and reduce the required amount of catalyst, thus leads to reduce the stack size and cost to power electronics.

3.3. Water electrolysis performance

For each of the three electrolyte systems (acid single electrolyte system, alkali single electrolyte system, and dual electrolyte system), its water splitting voltages were intersection points of the linear part of U-I curves and U-axis (Fig. 3a), and this can be determined by linear fitting its U-I curve and then calculating the U value when the I value is set to zero. Thus, the water splitting voltage was 1.495 V for the acid single electrolyte system, 1.415 V for the alkali single electrolyte system, and only 0.74 V for the duel electrolyte system, which was a great improvement. Since a lower water splitting voltage for water electrolysis system means less external power is required to break down water molecules and more power sources with much lower voltage can be utilized to split water and stored in the form of hydrogen energy and more power could be saved because of the low water splitting voltage. The primary reasons for the deviation of water splitting voltages from theoretical values were the same as those in FC mode discussed above. At a current density of 100 mA/cm², the cell could split water at a voltage of above 1.86 V in the alkali single electrolyte system and 2.05 V in acid single electrolyte system, while only 1.35 V in the DEFC which was not high enough for water to be split for the single electrolyte systems at any current densities.

As shown in Fig. 3b, the corresponding U-I curves of the cathode and anode for the DEFC followed the trend of the cathode in the single alkali electrolyte system, and the anode in the single acid electrolyte system as expected. This result revealed what the anode reaction and cathode reactions for the DEFC are (the same as Table 1). By adding up the two half-cell reactions, energy from the neutralization reactions was found to be counted as additional energy used to split water. Thus, as additional potentials from neutralization energy were applied to the electrodes, the potentials required to produce hydrogen and oxygen were lower than those in the single electrolyte systems, which contributed to a smaller decomposition voltage for the DEFC. If all neutralization energy has been converted to electrochemical energy, it could provide a voltage of 0.83 V to the electrodes, which is the same as

the difference of the water splitting voltage between the single (1.23 V) and dual electrolyte (2.06 V) in theory. In this mode, the neutralization energy utilization efficiency was calculated to be 9.7%, as shown in the supplementary material. This is the first time, to the best of our knowledge, that the energy from neutralization reactions was utilized directly as electrochemical energy to split water, instead of being wasted as heat in most situations.

3.4. Cycling efficiency and durability

Round-trip power efficiency in this case was evaluated by voltage efficiency [26], defined as the ratio of the discharge voltage (FC mode) to the charging voltage (WE mode) at a certain power density. As shown in Fig. 4a, relied on the dual electrolyte design, the efficiency of the DEFC was greatly improved compared with that of the single electrolyte system. The DEFC could still work with high efficiency at a high current density (even larger than 250 mA/cm²). At a current density of 50 mA/cm², a round-trip voltage efficiency of 127% was achieved for the DEFC. This value was greater than 100%, which was mainly attributed to the different pH environment of electrodes; the unique feature transferred the neutralization energy to electrical potential applied at the electrodes, thus improving the OCV and reducing the water splitting voltage. At a current density of 100 mA/cm², the roundtrip efficiency was 26.5% in the alkali single electrolyte system and 21.2% in the acid single electrolyte system; for the DEFC, however, the efficiency reached as high as 83.5%. Even at a current density of 200 mA/cm², the efficiency still stayed at about 36.8% while those values for the acid and alkali single electrolyte systems dropped to 3% and 2%, respectively.

The cycle performance of the device was evaluated for its durability. During a cycling test, the cell potential changes were monitored at various current densities (from 100 to 180 mA/cm²). As demonstrated in Fig. 4b, there is no observable performance degradation after 6 cycles' operation. In Fig. 4c, I-t curves of cycle performance of the DEFC are presented. Cycles were performed by using galvanostatic measurement at a current density of 121.2 mA/cm², and potentiostatic method at a voltage of 1 V. After repeatedly running cycles for about 1000 s, no significant degradation was observed.

The DEFC reported in this work has demonstrated decent electrochemical performance at room temperature under atmospheric pressure, which shows great potential of being a clean and

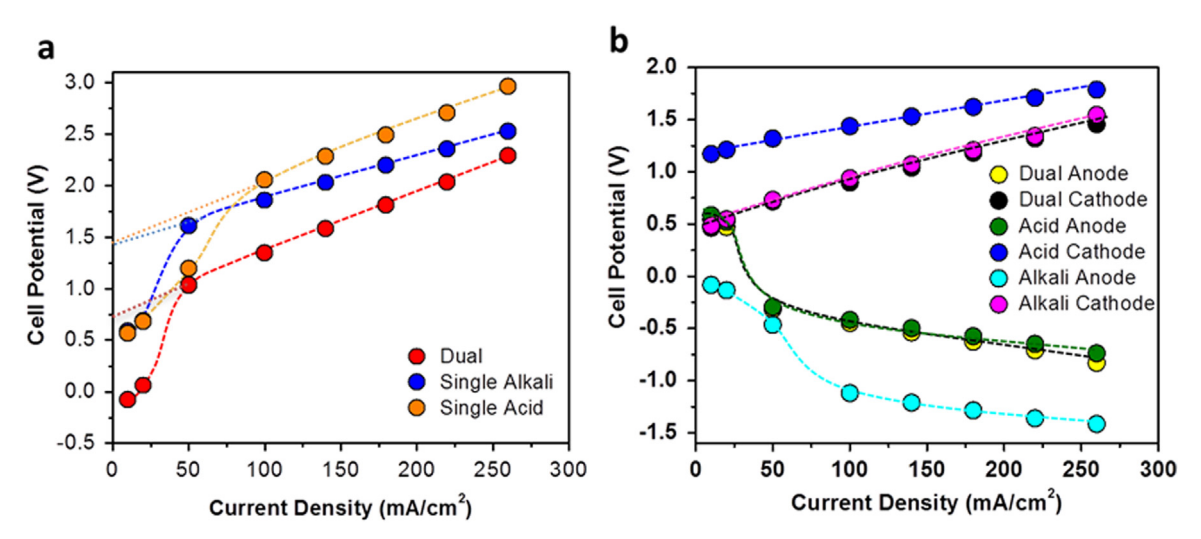


Fig. 3. Performance of the DEFCs in Water Electrolysis Mode. (a) Load curves comparison among the DEFC, fuel cell in single alkali system and single acid system. (b) The corresponding U-I curves of individual electrode performances versus Ag/AgCl.

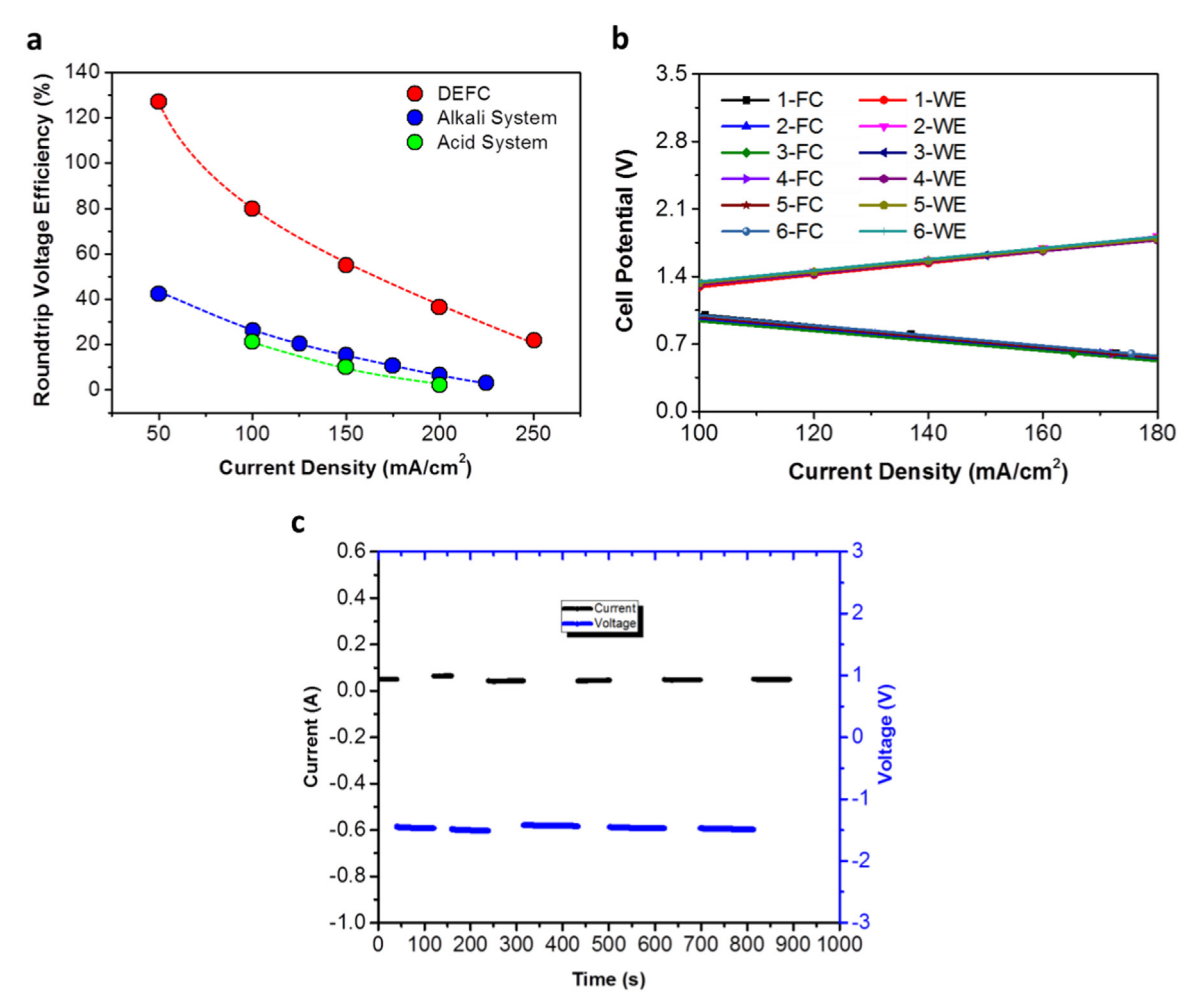


Fig. 4. Round-trip and cycle performance of the DEFC. (a) Round-trip voltage efficiency of the DEFC. The efficiency was greater than 100% in the DEFC due to the additional neutralization energy transferred to electrical potential applied at the electrodes. (b) Cycle performance of the DEFC. The cell potentials are at current density of from 100 to $180 \text{ mA} / \text{cm}^2$. (c) 1-t curves of cycle performance of the DEFC. Cycles were performed by using Galvanostatic (blue lines, current density= 121.2 mA/cm^2) and Potentiostatic (black lines, U=1 V) methods.

renewable energy technology. The technique also provides a great method to store low voltage energy efficiently like solar cells and a new method to store off-peak power for power stations to transfer electricity into hydrogen energy directly with a high efficiency. Since the stacking number of the systems can be reduced due to the higher power output and open circuit voltage the DEFCs produced. the amount of catalyst needed can be reduced, so the cost and size for the DEFCs' fabrication may be decreased. The membrane is avoided in this device. Fabrication of high-quality materials for membranes as well as the requirement of auxiliary systems for membrane has greatly increased the cost of FCs. More troubles are associated with the membrane in current designs, including humidification, membrane degradation, fuel crossover, packaging failure (due to the shrinkage and swelling of the membrane), and the challenge to keep a high proton conductivity of the membrane for different working operations [32,35]. Considering the cost of electrolytes, if industrial waste alkali and acid from factories are used as low-cost feed stocks, the cost would be relatively low, and the energy which is traditionally wasted as heat, now can be turned into useful energy to provide power and store energy, with no acidic or basic hazardous waste generated from the outlets finally. (Moreover, deleted) Further optimization of both single DEFC performance and integration of DEFC stacks in a recirculating fuel cell system could be the topic of future research.

4. Conclusion

This work represents a major advance of the state of the art in flow batteries as well as fuel cell system by reporting a rationally designed DEFC, which stably delivered an open circuit voltage up to 1.76 V at room temperature and atmospheric pressure. Creatively using a membraneless laminar flow-based electrolyte design in WE mode, the DEFC achieved a water splitting voltage of \sim 0.74 V, and a round trip voltage efficiency of as high as 83.5% at a current density of 100 mA/cm². Equipped with a commercialized catalyst, the DEFC ran stably, and exhibited a good cycling performance without observable degradation. The DEFCs could store the energy of low voltage electricity, and provide higher power than their single electrolyte counterparts. By decreasing fuel cell stack and eliminating the membrane and oxygen supplies system, the size of the DEFC and the cost to fabricate it were reduced. The neutralization energy was both experimentally and theoretically proved to be well utilized as electrochemical energy in dual electrolyte systems at the electrodes both in FC mode and WE mode. Holding a collection of compelling features such as roomtemperature operation, high open-circuit voltage, and low water splitting voltage, the DEFC technology presented in this work potentially renders a practical and effective approach to power portable electronics and large-scale electricity generation. This report opens a new window for both power sources and energy storage devices, and demonstrates that a dual electrolyte and pH

gradient or similar strategies might be used to achieve high electrochemical performance. Similar strategies like concentration differential and other advances in design and materials might also lead to achieving high electrochemical performance in other areas.

Acknowledgements

Haiyang Zou, Jun Chen, Yunnan Fang equally contributed to this work. The authors would like to acknowledge the financial support on this project from Hong Kong Research Grant Council GRF#714313. We thank Prof. Zhong Lin Wang, Prof. Meilin Liu for guidance and helpful suggestions. Haiyang Zou thanks Prof. Gleb Yushin, Prof. Dennis Y.C. Leung, Dr. Jin Xuan, Dr. Huizhi Wang and Yifei Wang for comments and advice on experiments.

Appendix A. Supplementary material

Supplementary data associated with this article can be found in the online version at http://dx.doi.org/10.1016/j.nanoen.2016.07.036.

References

- [1] B.C.H. Steele, A. Heinzel, Nature 414 (2001) 345-352.
- [2] L. Grande, E. Paillard, J. Hassoun, J.B. Park, Y.J. Lee, Y.K. Sun, S. Passerini, B. Scrosati, Adv. Mater. 27 (2015) 784–800.
- [3] J. Chen, G. Zhu, W.Q. Yang, Q.S. Jing, P. Bai, Y. Yang, T.C. Hou, Z.L. Wang, Adv. Mater. 25 (2013) 6094–6099.
- [4] N. Nitta, F.X. Wu, J.T. Lee, G. Yushin, Mater. Today 18 (2015) 252-264.
- [5] Z.L. Wang, J. Chen, L. Lin, Energy Environ. Sci. 8 (2015) 2250–2282.
- [6] Y.F. Hu, Z.L. Wang, Nano Energy 14 (2015) 3-14.
- [7] S.H. Wang, L. Lin, Z.L. Wang, Nano Energy 11 (2015) 436–462.
- [8] L. Carrette, K.A. Friedrich, U. Stimming, ChemPhysChem 1 (2000) 162–193.
- [9] H. Zou, E. Gratz, D. Apelian, Y. Wang, Green Chem. 15 (2013) 1183–1191.
- [10] J.R. Varcoe, Atanassov, D.R. Dekel, A.M. Herring, M.A. Hickner, A. Kohl, A. R. Kucernak, W.E. Mustain, K. Nijmeijer, K. Scott, T.W. Xu, L. Zhuang, Energy Environ. Sci. 7 (2014) 3135–3191.
- [11] M.L. Liu, M.E. Lynch, K. Blinn, F.M. Alamgir, Y. Choi, Mater. Today 14 (2011) 534–546.
- [12] C. Su, W. Wang, M.L. Liu, M.O. Tade, Z. Shao, Adv. Energy Mater. 5 (2015) 1500118.
- [13] U. Eberle, B. Muller, R. von Helmolt, Energy Environ. Sci. 5 (2012) 8780-8798.
- [14] H.R. Jhong, F.R. Brushett, J.A. Kenis, Adv. Energy Mater. 3 (2013) 589–599.
- [15] A. Atkinson, S. Barnett, R.J. Gorte, J.T.S. Irvine, A.J. Mcevoy, M. Mogensen, S. C. Singhal, J. Vohs, Nat. Mater. 3 (2004) 17–27.
- [16] Y.Y. Shao, G. Yin, Z.B. Wang, Y.Z. Gao, J. Power Sources 167 (2007) 235–242.
 [17] S. Bose, T. Kuila, X.L.N. Thi, N.H. Kim, K.T. Lau, J.H. Lee, Prog. Polym. Sci. 36
- (2011) 813–843.
- [18] I. Cowin, C.T.G. Petit, R. Lan, J.T.S. Irvine, S.W. Tao, Adv. Energy Mater. 1 (2011) 314–332.
- [19] R. Ferrigno, A.D. Stroock, T.D. Clark, M. Mayer, G.M. Whitesides, J. Am. Chem. Soc. 124 (2002) 12930–12931.
- [20] E.R. Choban, L.J. Markoski, A. Wieckowski, J.A. Kenis, J. Power Sources 128 (2004) 54–60.
- [21] R.S. Jayashree, L. Gancs, E.R. Choban, A. Primak, D. Natarajan, L.J. Markoski, J. A. Kenis, J. Am. Chem. Soc. 127 (2005) 16758–16759.
- [22] J.L. Cohen, D.A. Westly, A. Pechenik, H.D. Abruna, J. Power Sources 139 (2005) 96–105.
- [23] E. Kjeang, B.T. Proctor, A.G. Brolo, D.A. Harrington, N. Djilali, D. Sinton, Electrochim. Acta 52 (2007) 4942–4946.
- [24] E. Kjeang, R. Michel, D.A. Harrington, N. Djilali, D. Sinton, J. Am. Chem. Soc. 130 (2008) 4000–4006.
- [25] G. He, Z. Li, J. Zhao, S. Wang, H. Wu, M.D. Guiver, Z. Jiang, Adv. Mater. 27 (2015) 5280–5295.
- [26] W.A. Braff, M.Z. Bazant, C.R. Buie, Nat. Commun. 4 (2013) 2346.
- [27] Y.N. Zhang, H.M. Zhang, Y.W. Ma, J.B. Cheng, H.X. Zhong, S.D. Song, H. Ma, J. Power Sources 195 (2010) 142–145.
- [28] G.Y. Chen, S.R. Bare, T.E. Mallouk, J. Electrochem. Soc. 149 (2002) A1092–A1099.
- [29] Z.G. Shao, B.L. Yi, M. Han, J. Power Sources 79 (1999) 82-85.
- [30] F. Mitlitsky, B. Myers, A.H. Weisberg, Energy Fuels 12 (1998) 56–71.
- [31] W. Smith, J. Power Sources 86 (2000) 74-83.
- [32] E. Kjeang, N. Djilali, D. Sinton, J. Power Sources 186 (2009) 353–369.
- [33] C.K. Dyer, Fuel Cells Bull. 2002 (2002) 8–9.
- [34] J. Larminie, A. Dicks, M.S. McDonald, Fuel Cell Systems Explained, 2, Wiley,

- New York, 2003.
- [35] S.A. Mousavi Shaegh, N.-T. Nguyen, S.H. Chan, Int. J. Hydrogen Energy 36 (2011) 5675–5694.
- [36] M. Winter, R.J. Brodd, Chem. Rev. 104 (2004) 4245-4270.
- [37] S. Pennathur, J.C.T. Eijkel, A. van den Berg, Lab Chip 7 (2007) 1234–1237.
- [38] K.V. Kordesch, J. Electrochem. Soc. 125 (1978) C77-C91.
- [39] S. Srinivasan, Fuel Cells: From Fundamentals to Applications, Springer Science & Business media, Berlin, 2006.
- [40] J. Barrett, Inorganic Chemistry in Aqueous Solution vol. 21, Royal Society of Chemistry, London, 2003.
- [41] A.J. Bard, L.R. Faulkner, Electrochemical Methods: Fundamentals and Applications, Wiley, New York, 1980.
- [42] D.A. MacInnes, The Principles of Electrochemistry, Dover, New York, 1961.
- [43] E.R. Choban, J.S. Spendelow, L. Gancs, A. Wieckowski, J.A. Kenis, Electrochim. Acta 50 (2005) 5390–5398.
- [44] J.K. Norskov, J. Rossmeisl, A. Logadottir, L. Lindqvist, J.R. Kitchin, T. Bligaard, H. Jonsson, J. Phys. Chem. B 108 (2004) 17886–17892.
- [45] J.L. Cohen, D.J. Volpe, D.A. Westly, A. Pechenik, H.D. Abruna, Langmuir 21 (2005) 3544–3550.
- [46] A.B. Anderson, Electrochim. Acta 47 (2002) 3759–3763.
- [47] N.M. Markovic, H.A. Gasteiger, B.N. Grgur, N. Ross, J. Electroanal. Chem. 467 (1999) 157–163.
- [48] J.X. Wang, N.M. Markovic, R.R. Adzic, J. Phys. Chem. B 108 (2004) 4127-4133.
- [49] G.C. Li, G. Pickup, Electrochim. Acta 49 (2004) 4119–4126.
- [50] R.S. Jayashree, M. Mitchell, D. Natarajan, L.J. Markoski, J.A. Kenis, Langmuir 23 (2007) 6871–6874.



Haiyang Zou received his M.S. degree in Worcester Polytechnic Institute, United States in 2012 and B.S. degree in Nanchang University, China in 2010. He is currently a Ph.D. candidate in Georgia Institute of Technology under the supervision of Prof. Zhong Lin Wang. Haiyang's research interests include energy nanomaterials, nano-systems and nano-devices; peizoelectronics and piezo-optoelectronics, flexible electronics.

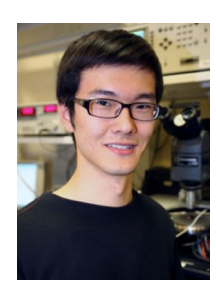


rent H-index is 34.

Jun Chen received his Ph.D. in Materials Science and Engineering from Georgia Institute of Technology in 2016. He is currently a postdoctoral researcher at Stanford University. His research focuses primarily on nanomaterial-based energy harvesting, energy storage, active sensing and self-powered micro-/nano-systems. He has already published 64 papers and 34 of them as first-author in prestigious scientific journals. And still, he filed 23 patents. His research on triboelectric nanogenerators has been highlighted by worldwide media over 400 times in total, including Nature, PBS, The Wall Street Journal, Washington Times, Scientific American, ScienceDaily, Newsweek, and so on. His cur-



Yunnan Fang is a research faculty in the School of Materials Science and Engineering at Georgia Institute of Technology, USA. He has obtained his B.Eng. from Southwest Jiaotong University, China in Metallic Materials, M.Sc from Tsinghua University, China and pH.D from Ohio State University, USA both in Biochemistry. His research focus on surface modification, bio-enabled and/or chemically-tailored fabrication of thin films and micro/nanoscale hierarchical 3-D structures/devices, formulation of inkjet inks, and inkjet printing of electronic devices. His work has been featured in over ten media outlets such as Science, Chemical & Engineering News, Chemistry World, and Headlines & Global News.



Jilai Ding is a Ph.D. candidate in School of Materials Science and Engineering, Georgia Institute of Technology. He received his B.S. degree from Zhejiang University, China in 2012. His research focuses on electrochemical and transport mechanisms in ionic conducting oxides on the nanoscale. Starting from Jan. 2015, he began conducting research in Oak Ridge National Laboratory, where he focuses on ionic conduction mechanisms of acceptor doped perovskites.



Ruiyuan Liu received his B.S. and M.S. degrees in Soochow University, China in 2011 and 2014. He is a Ph. D. candidate at Institute of Functional Nano and Soft Materials (FUNSOM), Soochow University. He is currently a visiting student in Prof. Zhong Lin Wang's research group at Georgia Institute of Technology, USA. His research interests include semiconductor nanostructures fabrication and application, solar cells, nanogenerators and self-powered nanosystems.



Wenbo Peng received his B.S. in Microelectronics from Xi'an Jiaotong University, China in 2010 and after that he started to pursue his Ph.D. degree in Electronic Science and Technology at Xi'an Jiaotong University. Now he is a visiting pH.D. student in School of Materials Science and Engineering at Georgia Institute of Technology under the supervision of Prof. Zhong Lin (Z. L.) Wang through the program of China Scholarship Council (CSC). His research interests mainly focus on piezotronics/piezo-phototronics, tribotronics, triboelectric nanogenerators and surface acoustic wave sensors.